

Supporting information for:

# **A Highly Conductive Conjugated Coordination Polymer for Fast-Charge Sodium-Ion Batteries: Reconsidering its Structures**

Yanchao Wu, Yuan Chen, Mi Tang, Shaolong Zhu, Cheng Jiang, Shuming Zhuo and Chengliang Wang\*

School of Optical and Electronic Information, Wuhan National Laboratory for Optoelectronics (WNLO), Huazhong University of Science and Technology, Wuhan 430074, China.

## **Experiential section**

**Synthesis of the CCPs Ni-TTO:** 1,3,4,6-tetrathiapentalene-2,5-dione (500 mg, 2.4 mmol) was reacted with excess amount of NaOMe (14.4 mmol, 6.0 eq.) in refluxed methanol for 24 hours. Then NiCl<sub>2</sub>·6H<sub>2</sub>O (424 mg, 2.4 mmol, 1 eq.) was dissolved in 20 mL degassed MeOH and the solution was added to the reaction mixture slowly, which lasted over 1 hour. The resulting mixture was kept reflux for 2 days. After cooled to room temperature, the black precipitate was collected by centrifugation and washed with MeOH, H<sub>2</sub>O and acetone successively. The obtained black product was extracted by Soxhlet extractor with methanol and acetone solution successively. The final products were dried under vacuum. Elemental analysis (%): C, 15.16; S, 43.13; H, 1.62. Inductively coupled plasma optical emission spectroscopy (ICP-OES) (%): Na, 2.77; Ni, 30.02. Theoretical (%): Ni, 27.82; C, 11.39; S, 60.79.

**Control experiments** were conducted to demonstrate the effect of exposure to air on the value x in the poly[Na<sub>x</sub>(Ni-TTO)]. Oxidized polymers were obtained by using the same procedure with the unoxidized polymers and followed by placing the final solution in air for 3 hours. The contents of Na and Ni were conducted by ICP-OES:

without exposure to air (%), Na, 5.15; Ni, 34.2; exposure to air for 3 hours (%), Na, 3.71; Ni, 32.8. The lower content of Na and the closer content of Ni to the theoretical value of Ni indicated that the exposure of the reaction solution is essential to achieving desired structure and the final chemical structure should be Ni-TTO.

### **Materials characterization**

Elemental analyses including C, H, and S were measured by a Vario Micro Cube Elemental Analyzer. The sodium and nickel contents were recorded in Agilent ICP-OES 730. XRD patterns were measured with a Cu-K $\alpha$  X-ray radiation source ( $\lambda = 0.154056$  nm) incident radiation by an X'Pert3 Powder instrument. The FT-IR spectra were recorded in the range 400–4,000  $\text{cm}^{-1}$  on Bruker ALPHA spectrometer. XPS measurements were carried out on a Thermo Fisher EscaLab 250Xi. EPR was carried out on Bruker A300 at low temperature (-77 K).

### **Electrochemical measurement**

The working electrodes were prepared by mixing the Ni-TTO (80 wt%) active materials with conductive additive super P (10 wt%) and sodium salt of carboxyl methyl cellulose (CMC) (10 wt%) in water solution. The slurry was coated onto aluminum foil and dried at 70 °C in vacuum overnight, giving a mass loading of Ni-TTO of about 2  $\text{mg cm}^{-2}$ . The 2032 coin cells were assembled in glove box with Ar atmosphere and 1 M NaPF $_6$  in DME was used as the electrolyte. GCD charge/discharge curves were performed in potential range of 1.2-3.2V on LAND CT2001A battery test system (Wuhan, China) at room temperature. Bio-logic VMP3 was used for cyclic voltammetry measurements, galvanostatic intermittent titration technique measurements and electrochemical impedance spectrum measurements. The electrodes for XPS and FT-IR measurements were prepared by polyvinylidene fluoride (PVDF) as binder. For the GITT measurement, the cells were charged and discharged at a current density of 0.1 A  $\text{g}^{-1}$  for a 5-min pulse and followed with a 30-min rest. The  $V_M$  (158.95  $\text{cm}^3\text{mol}^{-1}$ ) was obtained by measuring the mass and the total volume of a pressed Ni-TTO plate.

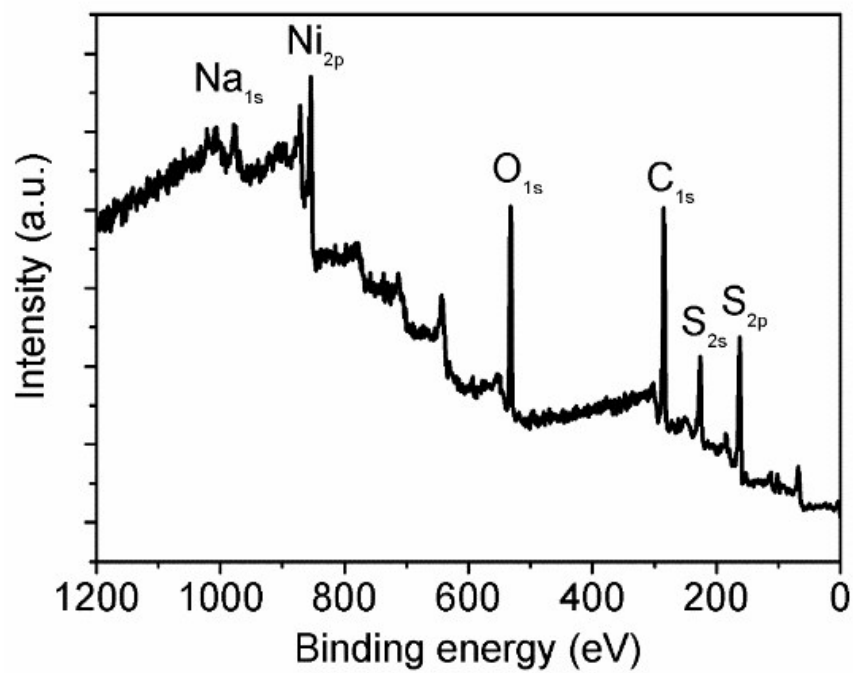


**Figure S1:** XPS spectra of the obtained Ni-TTO. The XPS spectra showed negligible counter cations of Na<sup>+</sup>, solidifying the proposed Ni-TTO structure.

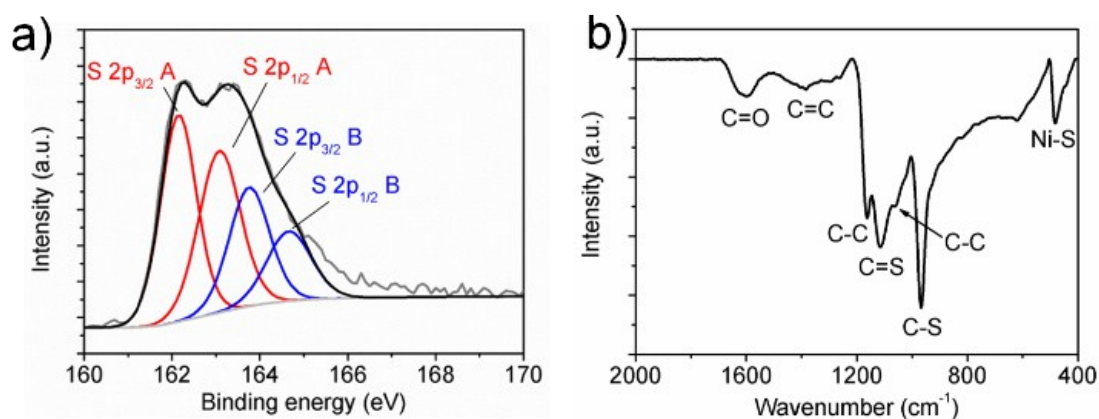


**Figure S2:** a) XPS spectra ( $S_{2p}$ ) and b) FT-IR spectra of the obtained Ni-TTO. The peaks located at  $1640\text{ cm}^{-1}$  can be assigned to the endcapping C=O groups. From the S 2p spectra, both the high valence states of S (B) and the low valence states (A) existed, which can be attributed to coexistence of C=S double bonds and C-S single bonds. From the FT-IR spectra, the absorption at  $\sim 1400$  and  $\sim 1163\text{ cm}^{-1}$  can be assigned to the C=C bond and C-C bond stretching respectively. The peak at  $\sim 1112\text{ cm}^{-1}$  probably belongs to the C=S bond stretching. The absorption at  $\sim 900\text{ cm}^{-1}$  can be identified to the C-S bond stretching. The peak at  $\sim 1000\text{ cm}^{-1}$  should be ascribed to the C-C bond bending. In addition, the peak at  $480\text{ cm}^{-1}$  can be assigned to Ni-S bonds. All of the results indicated the coexistence of C=S double and C-S single bonds, which can be ascribed to the resonance structure of Ni-TTO. The C-S bonds have partial double and partial single bond characters. Similarly, the C-C bonds also have the partial double bond and partial single bond characters.

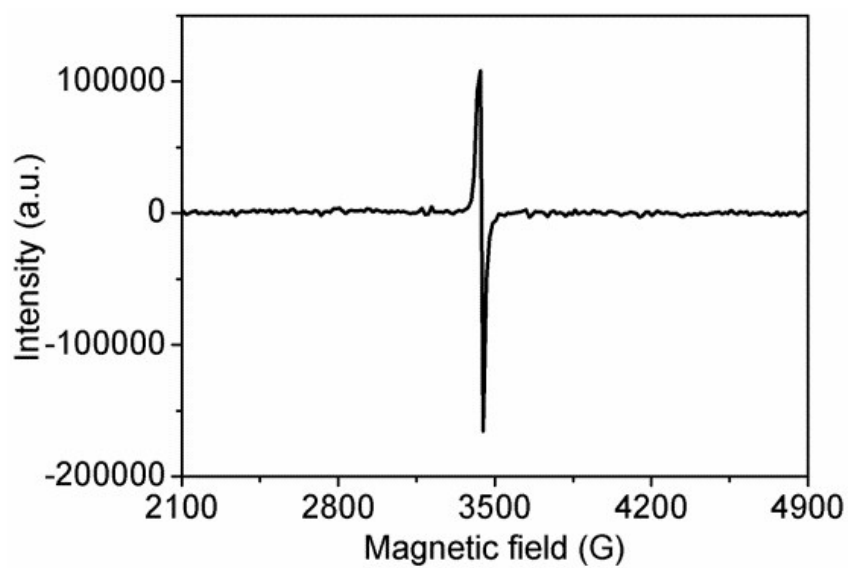


**Figure S3:** Electron paramagnetic resonance (EPR) spectra of the obtained Ni-TTO. The asymmetric EPR signal is a characteristic of radicals on the ligands, which agrees well with the proposed structure of Ni-TTO.

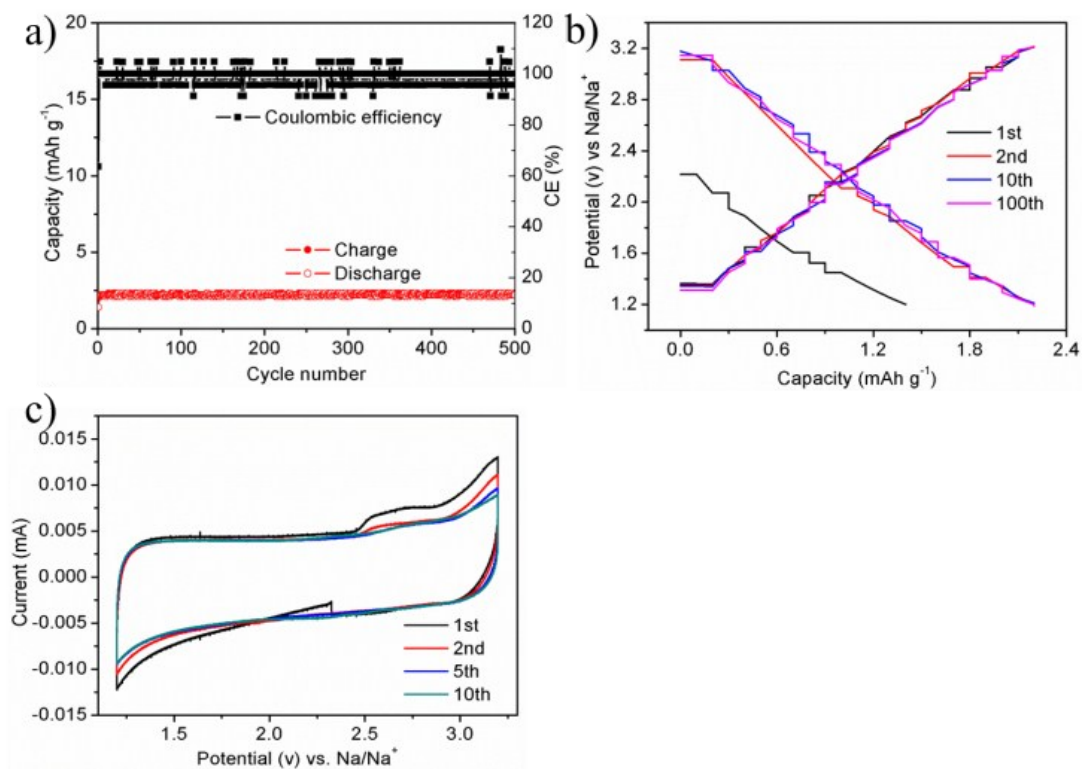


**Figure S4:** a) cycle performance of the conductive additive (Super P) at the current density of  $0.1 \text{ A g}^{-1}$ . (b) voltage-capacity curves of the electrode, the 1<sup>st</sup>, 2<sup>nd</sup>, 10<sup>th</sup>, 100<sup>th</sup> were selected as representatives. c) cyclic voltammetry curves of the Super P electrode between 1.2V to 3.2V. In view of the low content of super P in the electrodes (10 wt%), the capacity contribution of super P is negligible.

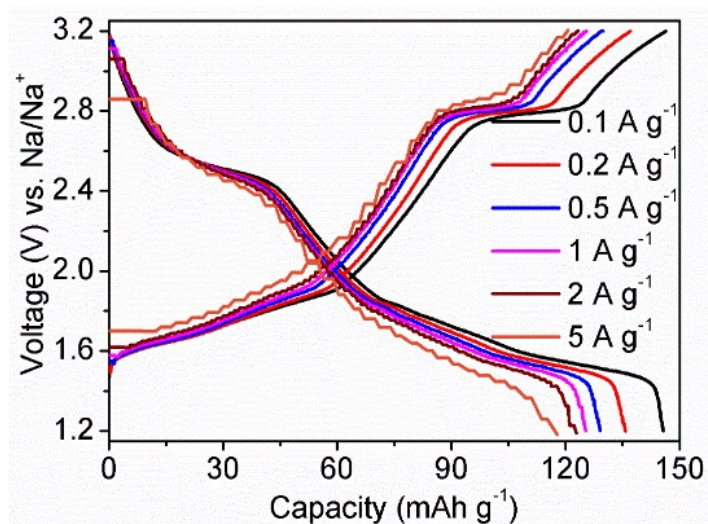


**Figure S5:** Voltage-capacity curves of the Ni-TTO electrodes when cycled at different current densities.

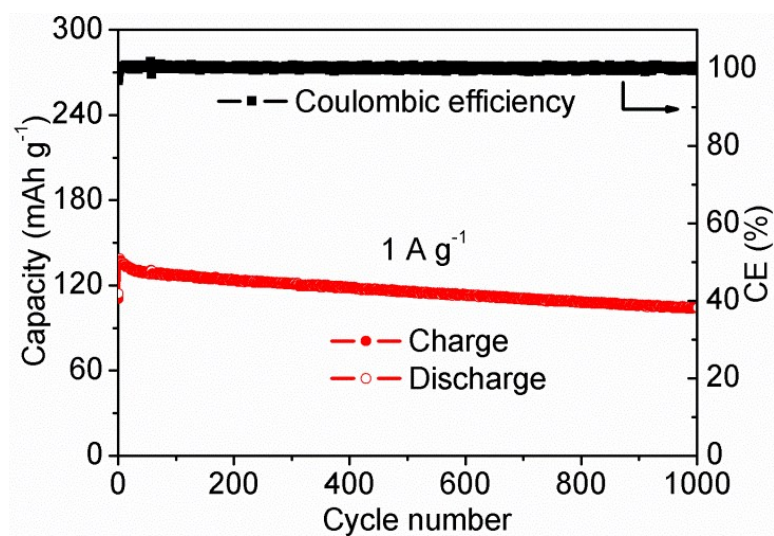


**Figure S6:** Long-term cycling performance of the Ni-TTO electrodes when cycled at a current density of 1 A g<sup>-1</sup>.

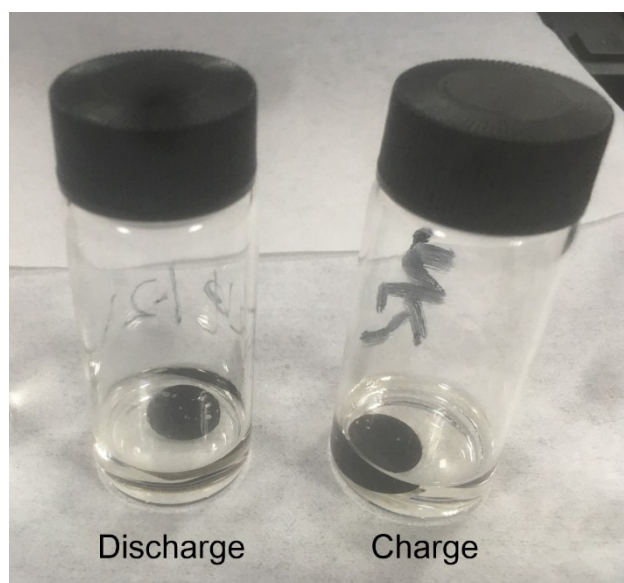
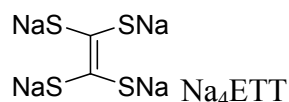


**Figure S7:** Optical images of the Ni-TTO electrodes after cycling.

### ESI-MS spectra of the discharged electrodes.

In order to check if the skeleton of the CCPs is stable during cycling, the ESI-MS spectra of the discharged samples were conducted. If the Ni-S bonds break during cycling, the most possible fragment of the CCPs should be:



Both the positive and negative modes were measured in the ESI-MS spectra. The measurements were conducted in solution of NH<sub>4</sub>OAc (0.1% in methanol). Therefore, the possible ESI-MS signals of the CCPs are listed in Table S1. Possible ESI-MS signals of NaOAc can also be observed, as shown in Table S2. From Figure S8 and Figure S11, the main peaks can be assigned to the NaOAc spices. The other peaks may come from the binder CMC-Na. What's more, we magnified all the areas that the ESI-MS signals of the CCPs may appear, and we found that all the possible spices of the fragments of the CCPs did not exist (Figure S9 and S12). Likewise, the signals of sulfides were also not observed (Table S3, Figure S10 and S13). These results indicated that the C-S-Ni bonds were probably stable during cycling.

**Table S1:** Possibility of ESI-MS signals (in positive and negative mode) for ETT fragments after being discharged.

Positive mode		Negative mode	
cation	u	anion	u
{Na <sub>5</sub> [ETT]} <sup>+</sup>	266.83	{Na <sub>3</sub> [ETT]} <sup>-</sup>	220.86
{Na <sub>5</sub> [ETT] + NaOAc} <sup>+</sup>	348.84	{Na <sub>3</sub> [ETT] + NaOAc} <sup>-</sup>	302.86
{Na <sub>5</sub> [ETT] + 2 NaOAc} <sup>+</sup>	430.84	{Na <sub>3</sub> [ETT] + 2NaOAc} <sup>-</sup>	384.86
{Na <sub>5</sub> [ETT] + 3 NaOAc} <sup>+</sup>	512.84	{Na <sub>3</sub> [ETT] + 3NaOAc} <sup>-</sup>	466.87
{Na <sub>5</sub> [ETT] + 4 NaOAc} <sup>+</sup>	594.85	{Na <sub>3</sub> [ETT] + 4NaOAc} <sup>-</sup>	548.87
{Na <sub>5</sub> [ETT] + 5 NaOAc} <sup>+</sup>	676.85	{Na <sub>3</sub> [ETT] + 5NaOAc} <sup>-</sup>	630.87

**Table S2:** Possibility of ESI-MS signals for NaOAc spices in positive and negative mode.

Positive mode		Negative mode	
cation	u	anion	u
{ Na [NaOAc]} <sup>+</sup>	104.99	{AcO [NaOAc]} <sup>-</sup>	141.02
{ Na [NaOAc] <sub>2</sub> } <sup>+</sup>	186.99	{AcO [NaOAc] <sub>2</sub> } <sup>-</sup>	223.02
{ Na [NaOAc] <sub>3</sub> } <sup>+</sup>	269.00	{AcO [NaOAc] <sub>3</sub> } <sup>-</sup>	305.02
{ Na [NaOAc] <sub>4</sub> } <sup>+</sup>	351.00	{AcO [NaOAc] <sub>4</sub> } <sup>-</sup>	387.02
{ Na [NaOAc] <sub>5</sub> } <sup>+</sup>	433.00	{AcO [NaOAc] <sub>5</sub> } <sup>-</sup>	469.03
{ Na [NaOAc] <sub>6</sub> } <sup>+</sup>	515.00	{AcO [NaOAc] <sub>6</sub> } <sup>-</sup>	551.03
		{AcO [NaOAc] <sub>7</sub> } <sup>-</sup>	633.03
		{AcO [NaOAc] <sub>8</sub> } <sup>-</sup>	715.04

**Table S3:** Possibility of ESI-MS signals for polysulfide spices in positive and negative mode.

Positive mode		Negative mode	
cation	u	anion	u
{Na <sub>3</sub> S} <sup>+</sup>	100.94	{NaS} <sup>-</sup>	54.96
{ Na <sub>3</sub> S + NaOAc} <sup>+</sup>	182.94	{NaS + NaOAc} <sup>-</sup>	136.96
{ Na <sub>3</sub> S + 2 NaOAc} <sup>+</sup>	264.94	{NaS + 2NaOAc} <sup>-</sup>	218.96
{ Na <sub>3</sub> S + 3 NaOAc} <sup>+</sup>	346.95	{NaS + 3NaOAc} <sup>-</sup>	300.97
{ Na <sub>3</sub> S + 4 NaOAc} <sup>+</sup>	428.95	{NaS + 4NaOAc} <sup>-</sup>	382.97
{ Na <sub>3</sub> S + 5 NaOAc} <sup>+</sup>	510.95	{NaS + 5NaOAc} <sup>-</sup>	464.97
		{NaS + 6NaOAc} <sup>-</sup>	546.98
		{NaS + 7NaOAc} <sup>-</sup>	628.98
		{NaS + 8NaOAc} <sup>-</sup>	710.98
		{NaS + 9NaOAc} <sup>-</sup>	792.99

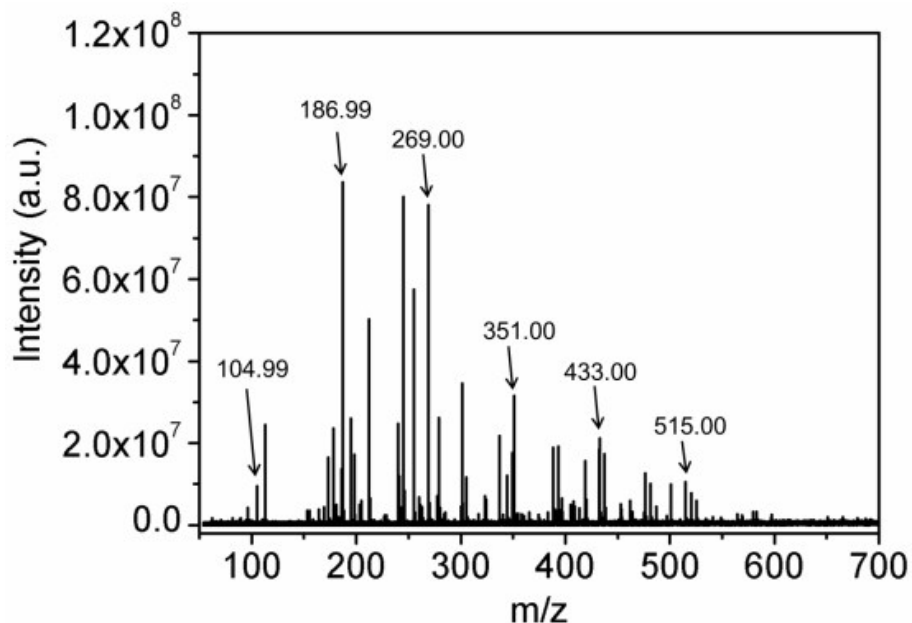


**Figure S8:** ESI-MS spectra (in positive mode in the solution of (MeOH, 0.1% of  $\text{NH}_4\text{OAc}$ )) of the electrodes after being discharged. The main peaks should be assigned to NaOAc species (see possibilities in Table S2). The other peaks may come from the binder CMC-Na.

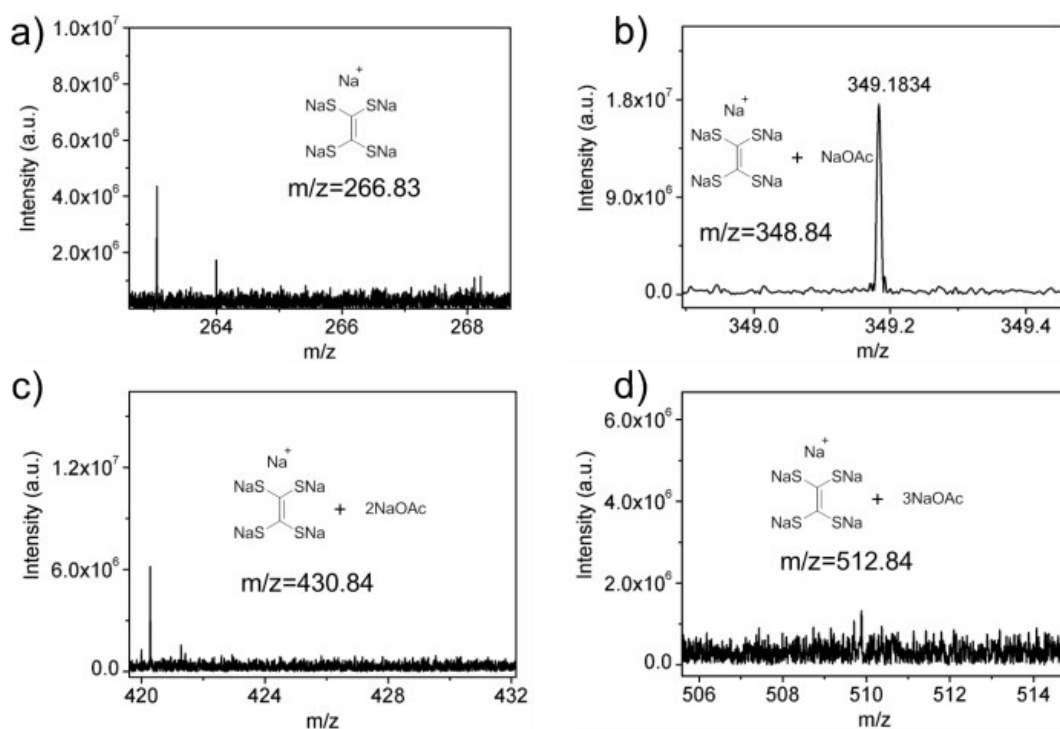


**Figure S9:** ESI-MS spectra (in positive mode in the solution of (MeOH, 0.1% of  $\text{NH}_4\text{OAc}$ )) of the electrodes after being discharged. No peaks can be assigned to the

ETT species (see possibilities in Table S1).

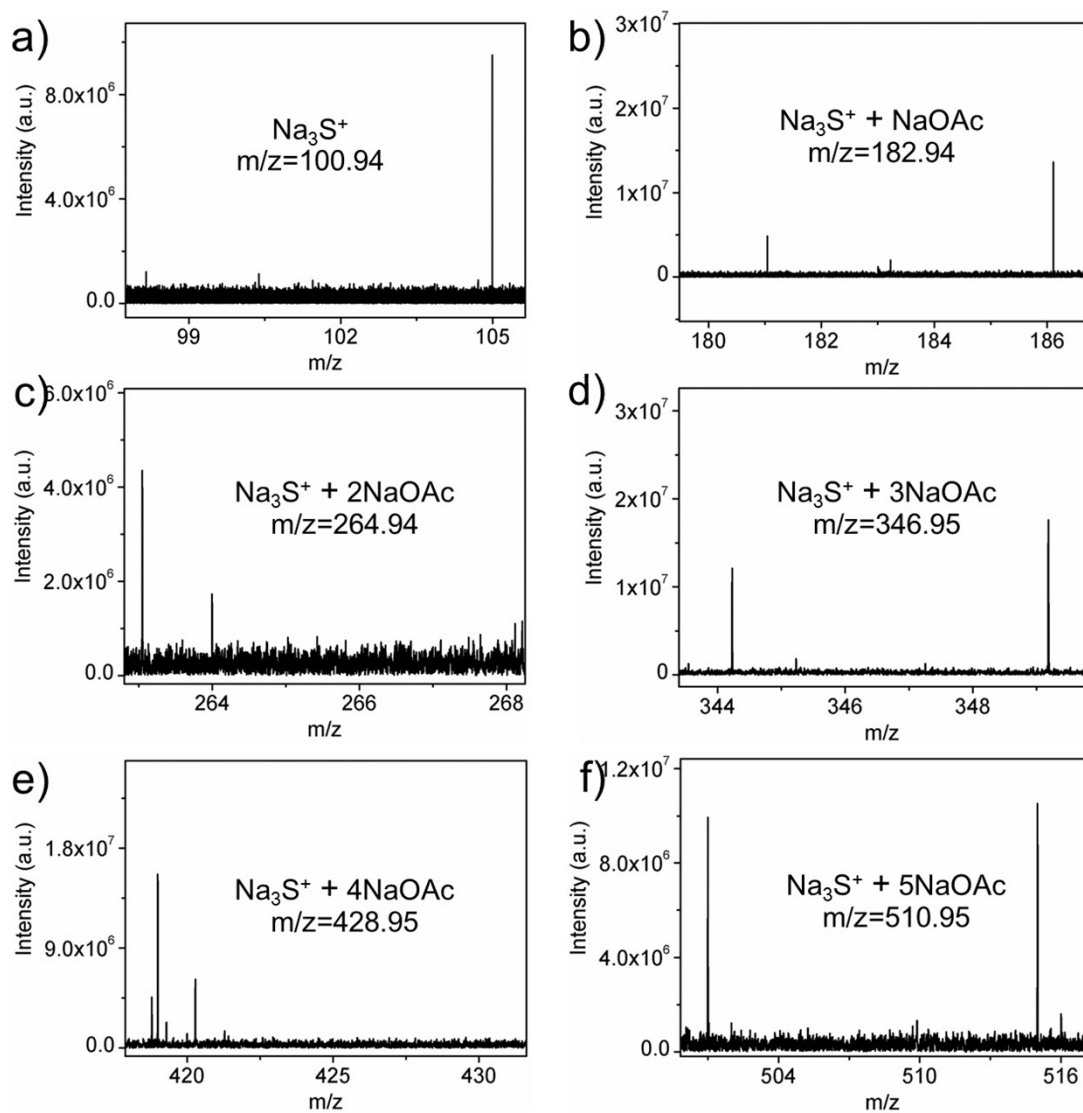


**Figure S10:** ESI-MS spectra (in positive mode in the solution of (MeOH, 0.1% of  $\text{NH}_4\text{OAc}$ )) of the electrodes after being discharged. No peaks can be assigned to the sulfide species (see possibilities in Table S3).

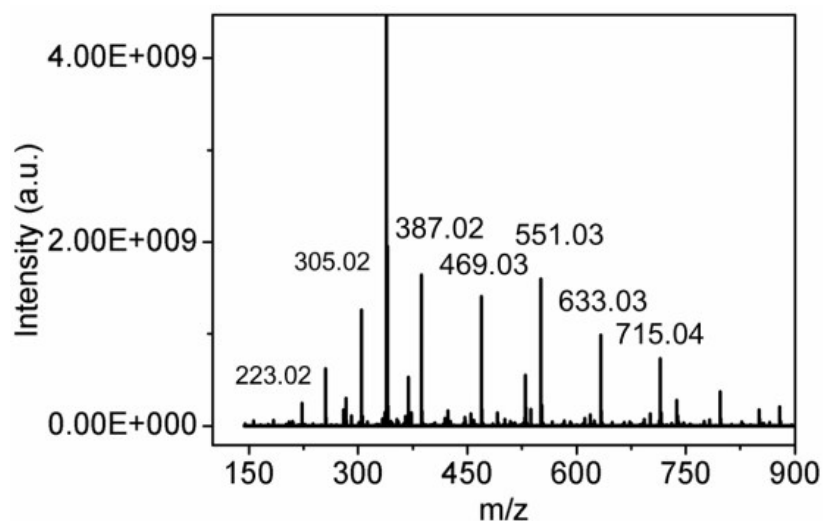


**Figure S11:** ESI-MS spectra (in negative mode in the solution of (MeOH, 0.1% of  $\text{NH}_4\text{OAc}$ )) of the electrodes after being discharged. The main peaks can be assigned to NaOAc species (see possibilities in Table S2). The other peaks may come from the binder CMC-Na.

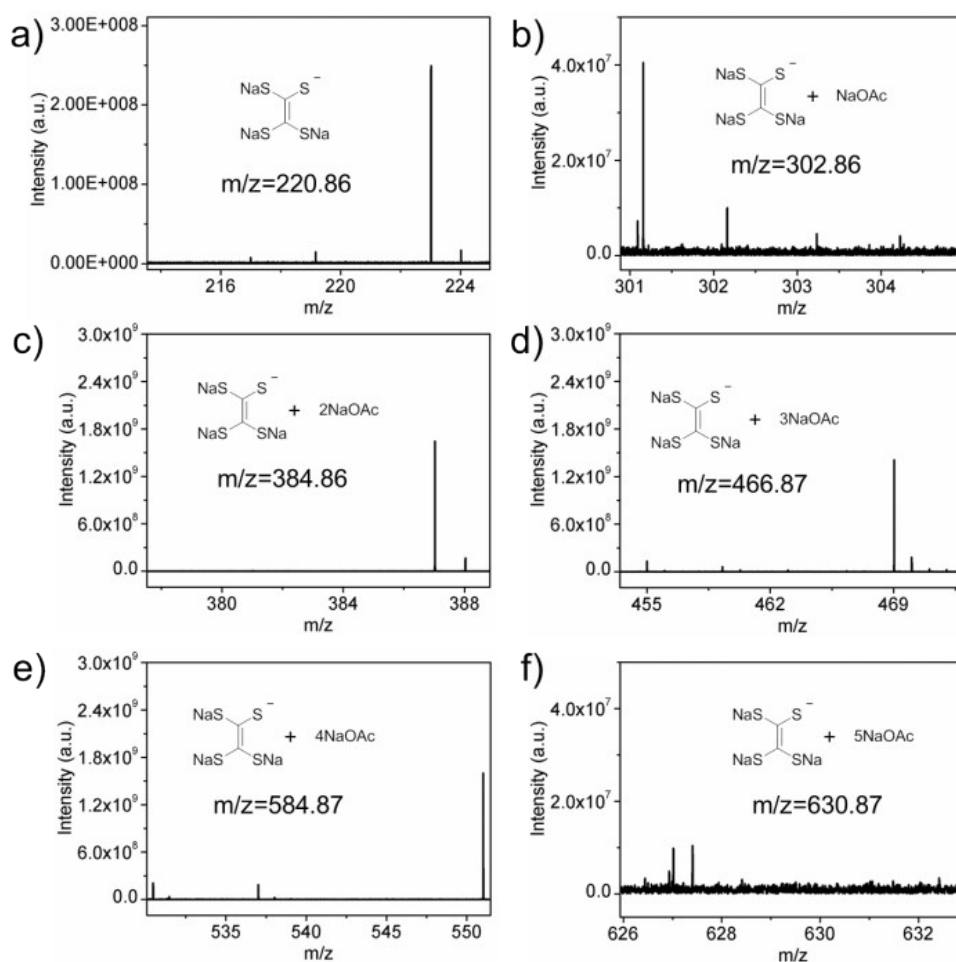


**Figure S12:** ESI-MS spectra (in negative mode in the solution of (MeOH, 0.1% of

NH<sub>4</sub>OAc)) of the electrodes after being discharged. No peaks can be assigned to the ETT species (see possibilities in Table S1).

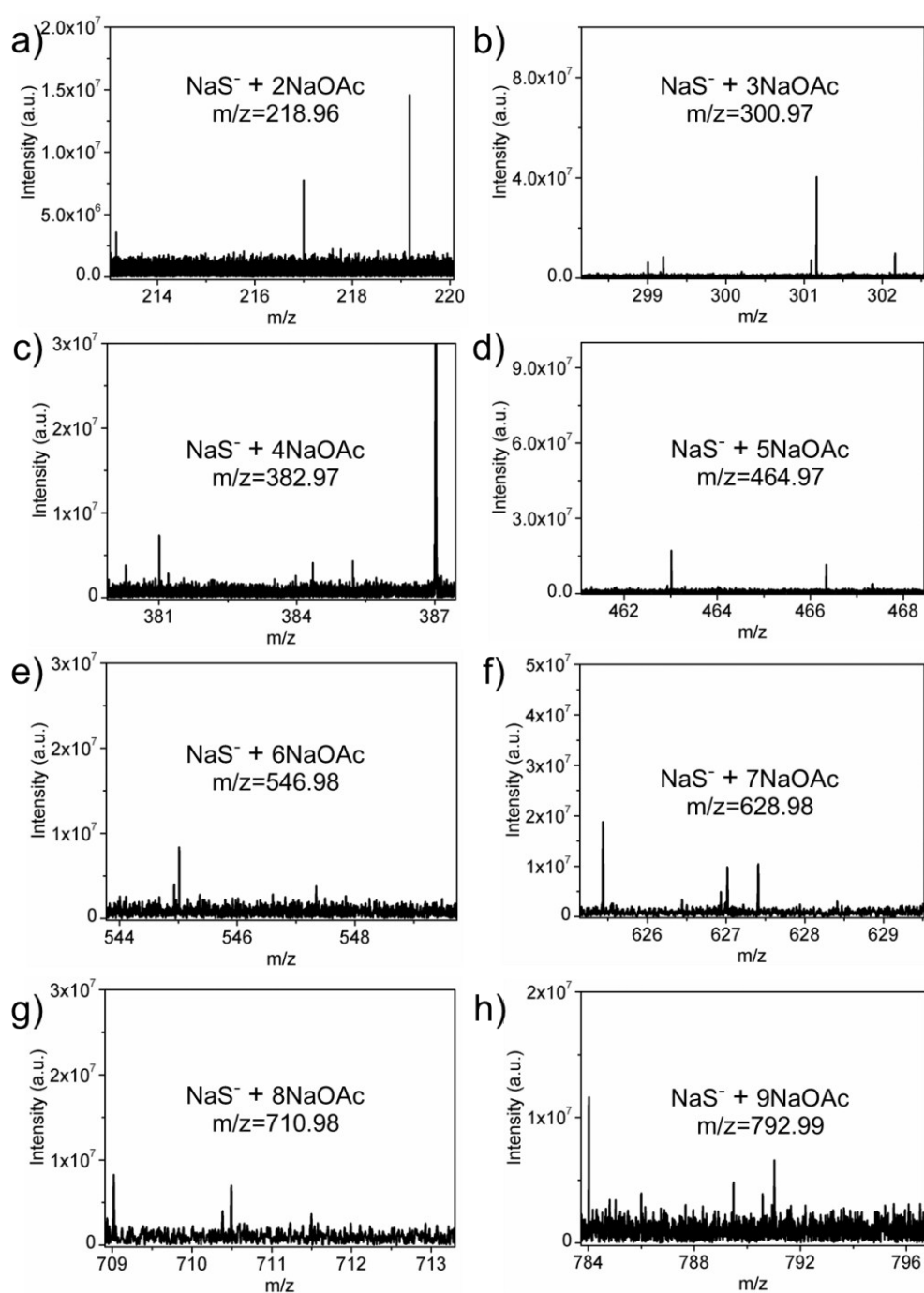


**Figure S13:** ESI-MS spectra (in negative mode in the solution of (MeOH, 0.1% of NH<sub>4</sub>OAc)) of the electrodes after being discharged. No peaks can be assigned to the sulfide species (see possibilities in Table S3).

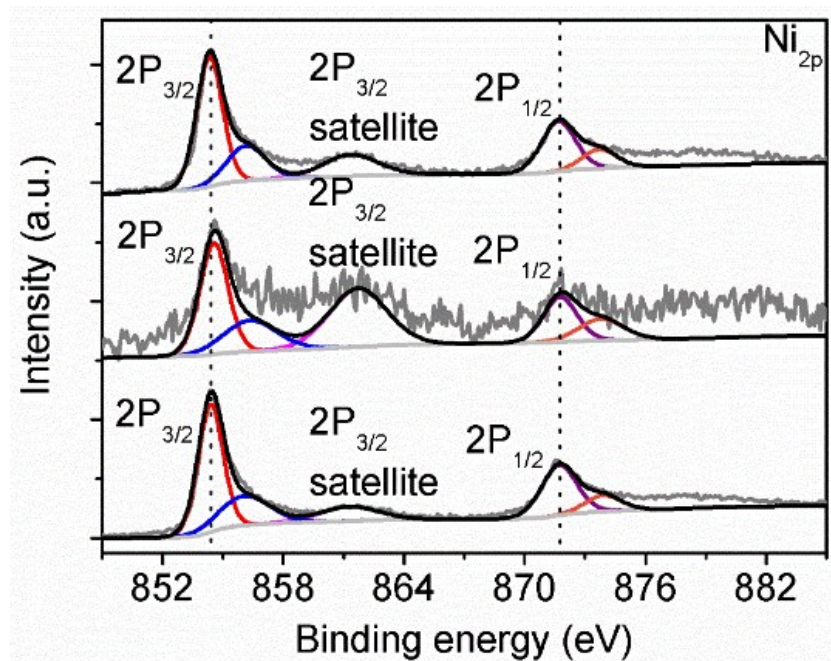


**Figure S14:** XPS spectra of Ni<sub>2p</sub> (from bottom to top: pristine and discharged to 1.2 V and recharged to 3.2 V, respectively). The Ni kept stable as valence of +2.

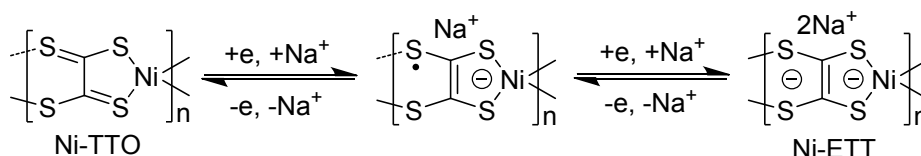


**Figure S15:** The proposed conversion mechanism of Ni-ETT and Ni-TTO, through redox reaction. The CV peaks showed two clear discharge peaks at 2.4 and 1.5 V, respectively. From the integral area ratio of the two main peaks (close to 1:1), the two peaks probably can be assigned to the two steps of reduction. In another word, the polymer Ni-TTO accepted one electron per repeating unit at about 2.4 V, accompanying with the insertion of one sodium ion. The electron is delocalized on the whole system and the system became negatively charged; hence the further acceptance of another electron and another sodium ion shifted to lower electrode potential of about 1.5 V. The presence of shoulder peaks and the fact that the integral area ratio of the two peaks was not exactly equal to 1:1 may be attributed to the existence of counter anions in Ni-TTO (indicating that some of the materials were already reduced into Ni-ETT) or the possible partial utilization of the active materials during cycling.

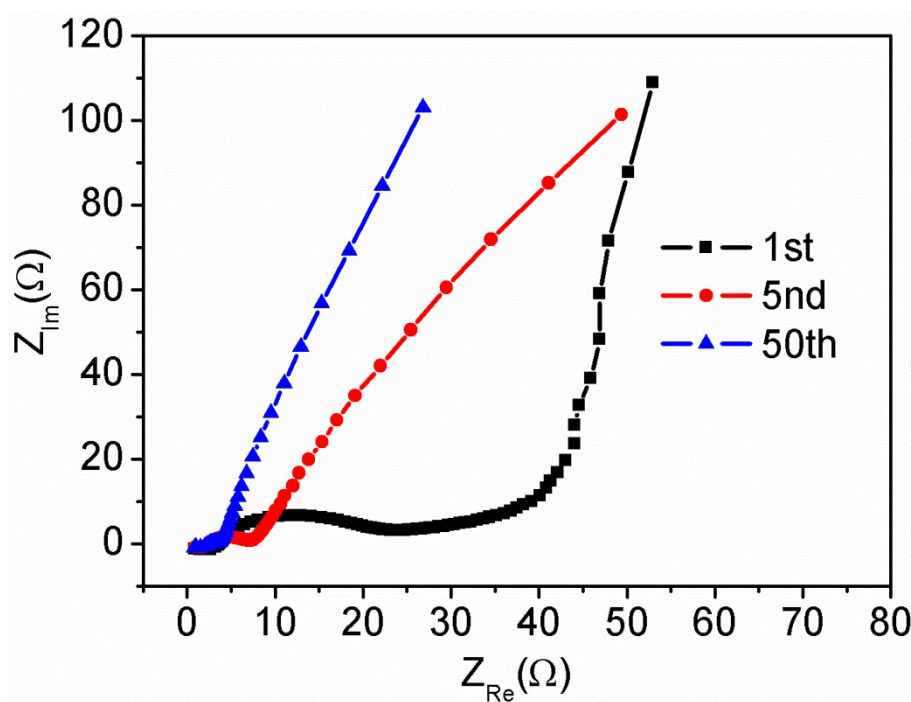


**Figure S16:** The EIS spectra of the Ni-TTO electrodes after discharging, the 1st, 5th,

50th cycles were selected as representatives.

**Table S4:** slope parameters of the log relationship of the absolute value of peak current and the scan rate.

Peak	A1	C1	A2	C2
Slope	0.97152	0.9202	0.86546	0.9471

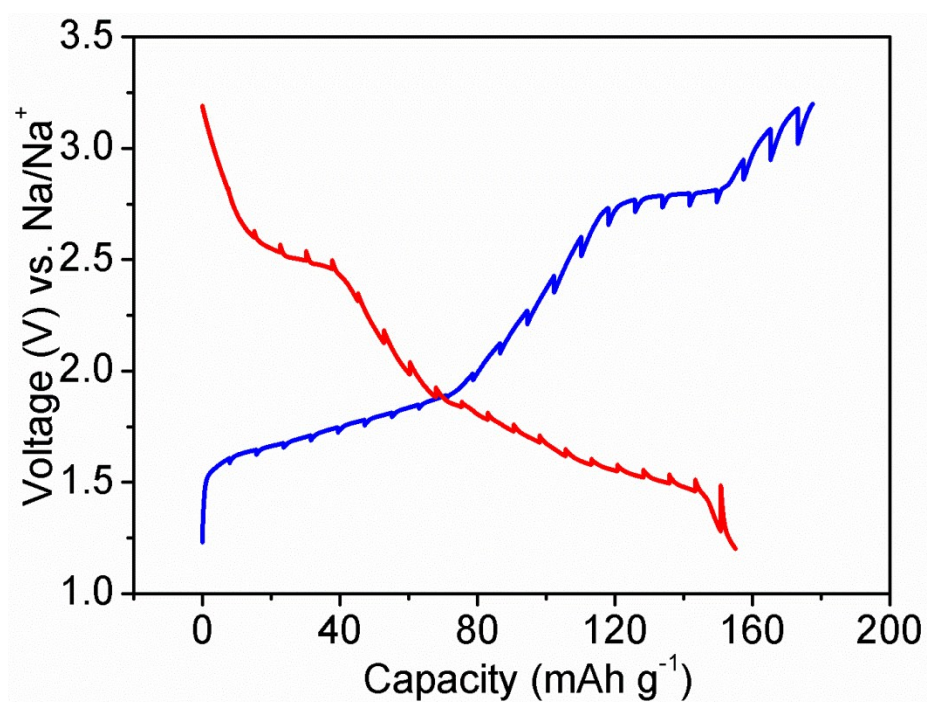


**Figure S17:** GITT potential response curve with time: a full discharge-charge cycle.



**Figure S18:** The  $V_M$  was obtained by calculated the mass and the total volume of a pressed Ni-TTO tablet.